

BROOKHAVEN NATIONAL LABORATORY

---

August 1997

RHIC DETECTOR NOTE

RHIC/DET Note 23

---

**Estimate of Dose Through Cracks  
in the STAR Shield Wall**

Alan J. Stevens

Brookhaven National Laboratory  
Upton, NY 11973

# Estimation of Dose Through Cracks in the STAR Shield Wall

## I. Introduction

An estimate of the dose through cracks in the STAR shield wall was previously made<sup>1</sup> using a series of approximations. For completeness, Ref. [1] is attached to this note as Appendix 2. Recently, this author acquired access to the LAHET Code System (LCS)<sup>2</sup> which is able, in principle, to calculate the dose through cracks without approximations other than, of course, the physics approximations in the particle production models within LCS. The general features of LCS, as well as its limitations, are described elsewhere.<sup>3</sup> Among those limitations are restrictions on computer time/space which implies that the (low energy neutron) dose estimates made here should be interpreted as the *excess dose* coming from the interior. The *total* dose should include other components of the dose as discussed in Ref. [1] (including the solid-wall dose estimate) which have been estimated using the CASIM program. Another limitation in LCS is the lack of the ability to include external magnetic fields. The results will be multiplied by 1.3 (the CASIM magnetic field enhancement factor near the midplane) as a correction for this effect.

## II. Geometry, Description of Calculations

A sketch of a part of the geometry is shown in Fig. 1. The wall shown is at the position of the STAR front shield wall. On either side of the front wall, in the actual design, are complicated regions including access labyrinths and shadow blocks, which are *not* simulated. In Fig. 1, the upstream one of these regions, is labeled "0 importance region." Transport for neutrons which enter this region is terminated. The geometry is cut off at the end of the front wall. The objective is therefore to calculate neutrons from the interior, including those which "reflect" off the ceiling and floor, through cracks in the front wall.

Also shown in Fig. 1 are three vertical cracks and MCNP "detectors" (the small black circles) behind the cracks. The upstream and downstream cracks are shown positioned in line with the "thick iron" of the magnet end pieces, which are the regions where allowance was made in Ref. [1] for additional dose. Behind the most upstream crack are two detectors, one 15 cm. behind the wall centered on the crack, and one displaced to the side by 15 cm. This second detector was positioned in that manner at one crack location to test the fall-off in the direction perpendicular to the crack direction. One of the assumptions in Ref. [1] was that this fall-off is very significant, so that the dose estimate could be "discounted" by a factor of 3 relative to whole body dose.

Unlike CASIM, LCS does not allow the initial interaction point to be smeared. Each LCS run is therefore at a single point in the beam pipe. The objective was to make a reasonable approximation of varying both the position of interaction (in the beam direction) and the crack location/orientation. In all cases, the primary interaction was taken as 100 GeV/c neutrons. An Au beam fault is approximated by the interaction of  $2.24 \times 10^{13}$  neutrons which is the number of nucleons at twice design intensity (one half of 4 times design intensity).

For each interaction point and configuration of cracks/detectors, some number ( $\geq 3$ ) of LCS "runs" were made varying the initial random number seed with at least 300 primary neutrons per run. The error is taken to be simply the estimate of  $\sigma$  from the multiple runs. In cases where the dose is very low, the statistical precision (limited by available file space) with such a small number of primaries is not sufficient to obtain a good estimate; the rms. of the multiple runs can exceed the mean value.

In the coordinate system used, the origin in the Z (beam) direction is taken to be the beginning of the DX magnet (see Appendix 1). In this system, the tunnel wall leading into the 6 o'clock hall is at  $Z = 550$  cm. The shield wall begins at  $Z = 806$  cm and ends at 1842 cm. The two "thick steel" sections of the magnet are in the range  $1018 \leq Z \leq 1068$  and  $1632 \leq Z \leq 1682$ .

### III. Results for Vertical Cracks

In the first set of runs, the shield wall shown in Fig. 1 was taken to be cylindrically symmetric. Three vertical cracks (actually *radial* with the cylindrical geometry) as illustrated in Fig. 1 were positioned at Z coordinates of 1020, 1350, and 1680 cm., each 3/8 inches wide. Referring to the coordinate system described above, the first of these cracks was near the beginning of the upstream thick steel section, and the third crack near the end of the downstream thick steel section. The detectors shown in Fig. 1 in this case are "ring detectors." With this set of cracks the source point was varied within the DX magnet. Points at 1/4, 1/2, and 3/4 along the length of DX were selected as a reasonable approximation of a "scraping loss." Fig 2 shows the results of this series of calculations. This figure shows (1) the dose exterior to crack1 and crack3 (at the thick iron positions) is indeed somewhat higher than the crack in the middle, (2) no dependence on the interaction position within DX is observed, and (3) statistics are not overly impressive.<sup>4</sup>

The result for the detector displaced by 15 cm. in the beam direction from the detector behind crack 1 was  $9.0 \pm 21 \times 10^{-17}$  rem/neutron. Although this is nominally an order of magnitude lower than the dose aligned with the crack, the statistical precision is very poor.

In an attempt to increase statistical precision, the gaps were opened to 1 inch. Runs were made which were consistent in all cases with the dose scaling linearly with the crack width. For crack1, for example, the dose for the 1 inch crack was  $2.17 \pm 0.28 \times 10^{-15}$  rem/p, in comparison to the average in Fig. 2 of  $9.6 \pm 1.6 \times 10^{-16}$  for the 3/8" crack width. The results for the displaced crack in this case was  $6.0 \pm 2.0 \times 10^{-17}$  rem/neutron. This result was taken as sufficient verification of the "discounting" of dose through a crack relative to whole body dose mentioned in Section I above; no further runs were made with a displaced detector. The remainder of the runs examining dose through vertical cracks was done with 1 inch wide cracks.

The next series of runs changed the neutron interaction point to positions on the beam pipe downstream of DX. The results are shown for the two cracks with the highest dose in Fig.

3. The first point in this figure has the source at the midpoint position in DX. The worst case is the first crack for the source on DX.<sup>5</sup>

The next series of runs moved the positions of the cracks along the shield wall searching for the worst case position. In this case the source was simply the middle of the DX magnet. As shown in Fig. 4, the "search points" were clustered more closely on the thick iron regions. The worst case was found was at a Z location corresponding to the middle of the first thick iron region, where the dose is estimated to be  $2.3 \pm .21 \times 10^{-15}$  rem/n for a 1 inch wide crack.

In preparation for the study of horizontal cracks, the geometry was changed to be rectangular, where the backwall, ceiling etc. are in the proper location with respect to the wall. The "ring detectors" in the cylindrical geometry become "point detectors" in a rectangular geometry. The runs described in the preceding paragraph were repeated with the same results. The result for the worst case position was (fortuitously)  $2.3 \pm .19 \times 10^{-15}$  rem/n.

To compare with the allowance made in Ref. [1], this result must be multiplied by 3/8 to "go back" to the 3/8 wide crack, by 1.3 to allow for a left-right magnetic field enhancement, and by 2 to allow for an increased quality factor for neutrons. The maximum fault dose is then:

$$2.3 \times 10^{-15} \times 3/8 \times 1.3 \times 2 \times 2.24 \times 10^{13} = 5 \times 10^{-2} \text{ rem} = 50 \text{ mrem.}$$

This is to be compared with the maximum allowance of about 1500 mrem<sup>6</sup> made in Ref. [1].

#### IV. Results for Horizontal Cracks

The STAR front wall design is such that the horizontal crack nearest the midplane is 45.7 cm. (18") from the midplane. A horizontal crack was placed at this position and another at 200 cm. from the midplane for comparison. Again, runs were made to explore dependence on the locations of both the source and position behind the wall.

In the first set of runs, the horizontal crack width was set at 1 inch and a series of runs were made with the source on the beam pipe in the middle of DX and point detectors at various Z locations behind the wall. The results of these runs are shown in Fig. 5. Clearly the horizontal crack nearest the midplane is (as expected) the worst case.

In the next set of runs the crack size was reduced to 3/16 inch and the source position within the DX magnet was varied. Fig. 6 shows results for the crack at Y = 45.7 cm at the position of the maximum (Z=1650, see Fig. 5). All the Z positions of the dose showed a modest dependence on the DX source location as illustrated in Fig. 6. Also, all the results are somewhat smaller than 3/16 of the 1" dose.

Two additional runs were made in an attempt to further explore the source location dependence. The first run was simply moving the source location to Z=750, a point on the beam

pipe downstream of DX. The result behind at the wall at  $Z = 1650$  reduced to  $1.2 \pm .07 \times 10^{-16}$  rem/n, continuing the "trend" shown in Fig. 6. To check the other direction required considerably more effort, namely changing the geometry to include an approximation of the D0 magnet upstream of DX. This magnet was approximated as it has been in CASIM estimates; it is placed as if DX and D0 were centered on a single beam line. The result (for an interaction point in the middle of D0, the only runs made) was that the  $Z = 1650$  position, although still the maximum, drops to  $2.13 \pm .7 \times 10^{-16}$  rem/n from the  $4.57 \pm .28 \times 10^{-16}$  rem/n shown for the source point at the upstream part of DX shown in Fig. 6.

This point will be taken as the worst case. Applying the same factors as in the case of vertical cracks, the excess dose in the canonical fault for a 3/16" horizontal crack is:

$$4.57 \times 10^{-16} \times 1.3 \times 2 \times 2.24 \times 10^{13} = 2.7 \times 10^{-2} \text{ rem} = 27 \text{ mrem}$$

Again, this is much smaller than the allowance of about 100 mrem "equivalent whole body" or 300 mrem in Ref. [1].

## V. Summary/Conclusion

Excess dose due to low energy neutrons through cracks in the STAR shield wall have been estimated using the LAHET Code System. This is a much better estimate than had been obtained previously.<sup>1</sup> The dose was found to be very small, about 50 mrem for a 3/8" vertical crack and 27 mrem for a 3/16" horizontal crack.

The allowance for the possibility of a thick iron effect in Ref. [1] was clearly greatly exaggerated. From this allowance the recommendation was made that two specific cracks in the STAR shield wall should be covered with polyethylene. This recommendation is not supported by the estimates described here.

It should be noted that there are other components of the total dose estimated in Ref. [1] (Appendix 2 of this document) that are present and for which the estimate in Ref. [1] remains valid, namely a "no-crack" component and "high energy" component due to the existence of the crack(s), both of which were estimated using the CASIM program. For the STAR shield wall these were 267 mrem (solid wall), 17 mrem for 3/8" vertical crack, and 7 mrem for a 3/16" horizontal crack (sufficiently removed from the midplane).

## References/Footnotes

1. A.J. Stevens, "Analysis of Cracks in the STAR Shield Wall," (unpublished). This document is an attachment to a Radiation Safety Committee, sub-committee meeting of 20 August, 1996 and is in the RSC files.

2. R.E. Prael and H. Lichtenstein, "User Guide to LCS: The LAHET Code System," Los Alamos National Laboratory Report LA-UR-89-3014, September, 1989.
3. A.J. Stevens, "Comparison of CASIM with the LAHET Code System," RHIC/AD/RD-115, August, 1997.
4. The rms. deviation on the crack in the middle position at the downstream interaction point exceeded the mean value and is not shown.
5. This is more true than apparent from Fig. 3 since the nominal dose for the source on DX must be multiplied by 1.3 for the magnetic field enhancement on the midplane.
6. In Ref. [1], the allowance for the low energy portion near the "thick iron" poles was 504 mrem equivalent whole body dose. The result here has no factor of 3 "discounting." Over most of the wall, the (conservative) estimate in Ref. [1] (Appendix 2) was about 180 mrem (equivalent whole body of 61 mrem), still over a factor of 3 greater than the current estimate.

## Appendix 1

All the calculations described in the text assumed a source due to interacting neutrons which are parallel to the tunnel direction on the beam pipe. The material in the DX magnet is simply described by a radial distribution along the magnet's magnetic length. The radial regions are shown in the table below.

**Table A-1 Radial Material Distribution in the DX Magnet**

| Region | Inner Radius<br>(cm.) | Outer Radius<br>(cm.) | Material<br>Description       |
|--------|-----------------------|-----------------------|-------------------------------|
| 1      | 0.000                 | 6.984                 | Vacuum                        |
| 2      | 6.984                 | 7.114                 | Beam pipe, warm bore, Steel#2 |
| 3      | 7.114                 | 8.140                 | Vacuum                        |
| 4      | 8.140                 | 8.700                 | Beam pipe, cold bore, Steel#2 |
| 5      | 8.70                  | 9.00                  | He Region                     |
| 6      | 9.00                  | 10.20                 | Coil                          |
| 7      | 10.20                 | 14.20                 | Collar, Steel#2               |
| 8      | 14.20                 | 31.20                 | Yoke, Steel #1                |
| 9      | 31.20                 | 38.40                 | Vacuum                        |
| 10     | 38.40                 | 39.00                 | Cryo. Vessel wall, Steel#3    |

The materials (e.g, Steel#1 etc.) are described further in Appendix A of Ref. [3]. See this reference also for the approximation of (light) concrete used in the walls of this calculation.

The steel warm bore beam pipe extends from the beginning of DX to a point 385 cm. upstream of the crossing point, after which an aluminum beam pipe in the radial range  $3.62 \leq R \leq 3.78$  cm. is assumed.

Near the end of the calculations described in the text, an approximation of the D0 magnet was added upstream of DX, separated from DX by a 7m free space. The material distribution in D0 is somewhat simpler, and is given in Table A-2 below

**Table A-2 Radial Material Distribution in the D0 Magnet**

| Region | Inner Radius<br>(cm.) | Outer Radius<br>(cm.) | Material<br>Description       |
|--------|-----------------------|-----------------------|-------------------------------|
| 1      | 0.00                  | 5.20                  | Vacuum                        |
| 2      | 5.20                  | 5.38                  | Beam pipe, cold bore, Steel#2 |
| 5      | 5.38                  | 5.40                  | He Region                     |
| 6      | 5.40                  | 6.40                  | Coil                          |
| 7      | 6.40                  | 7.40                  | Spacer (See Ref. [3])         |
| 8      | 7.40                  | 15.40                 | Yoke, Steel #1                |

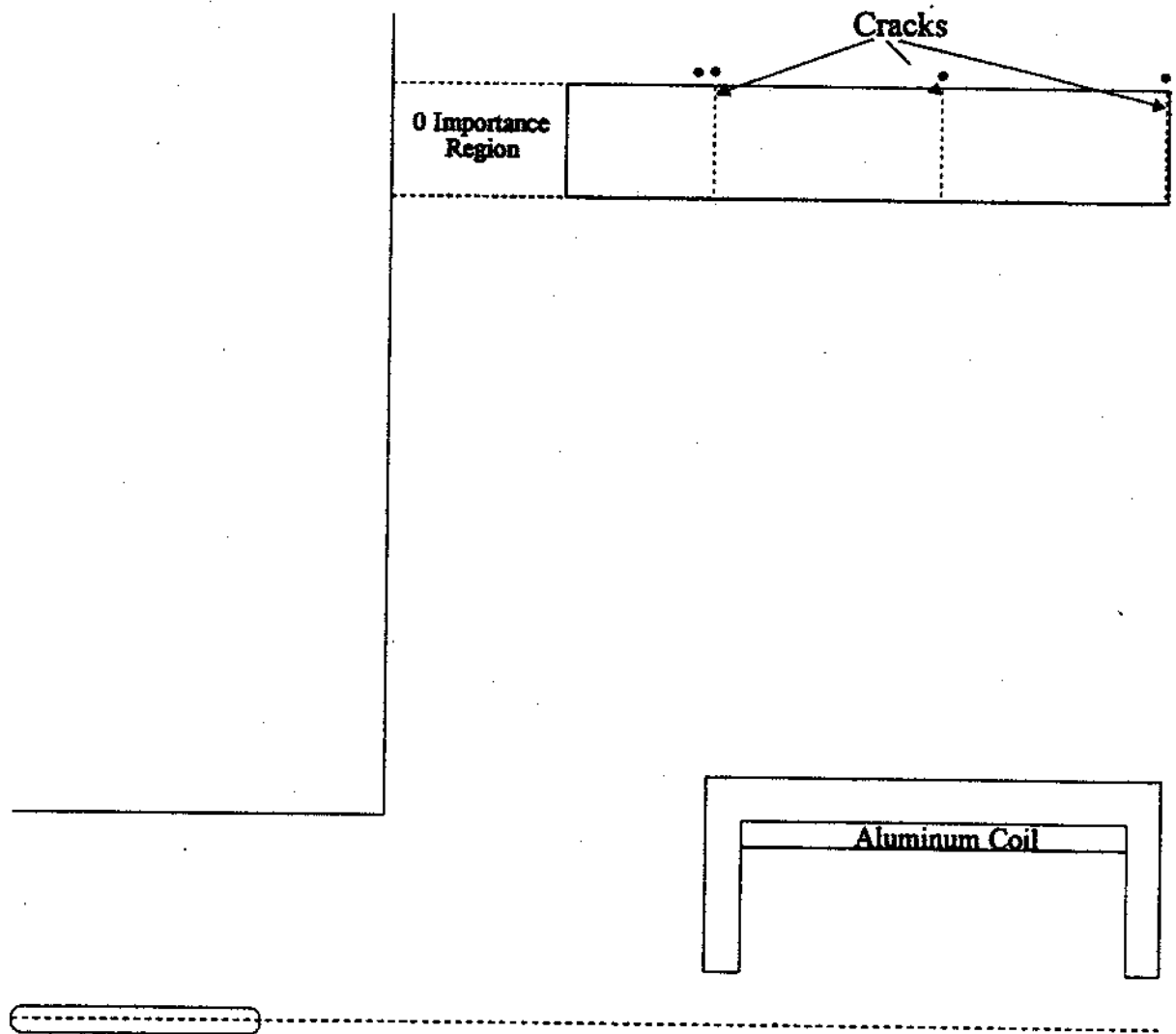


Fig. 1 Plan View of a Part of the Geometry

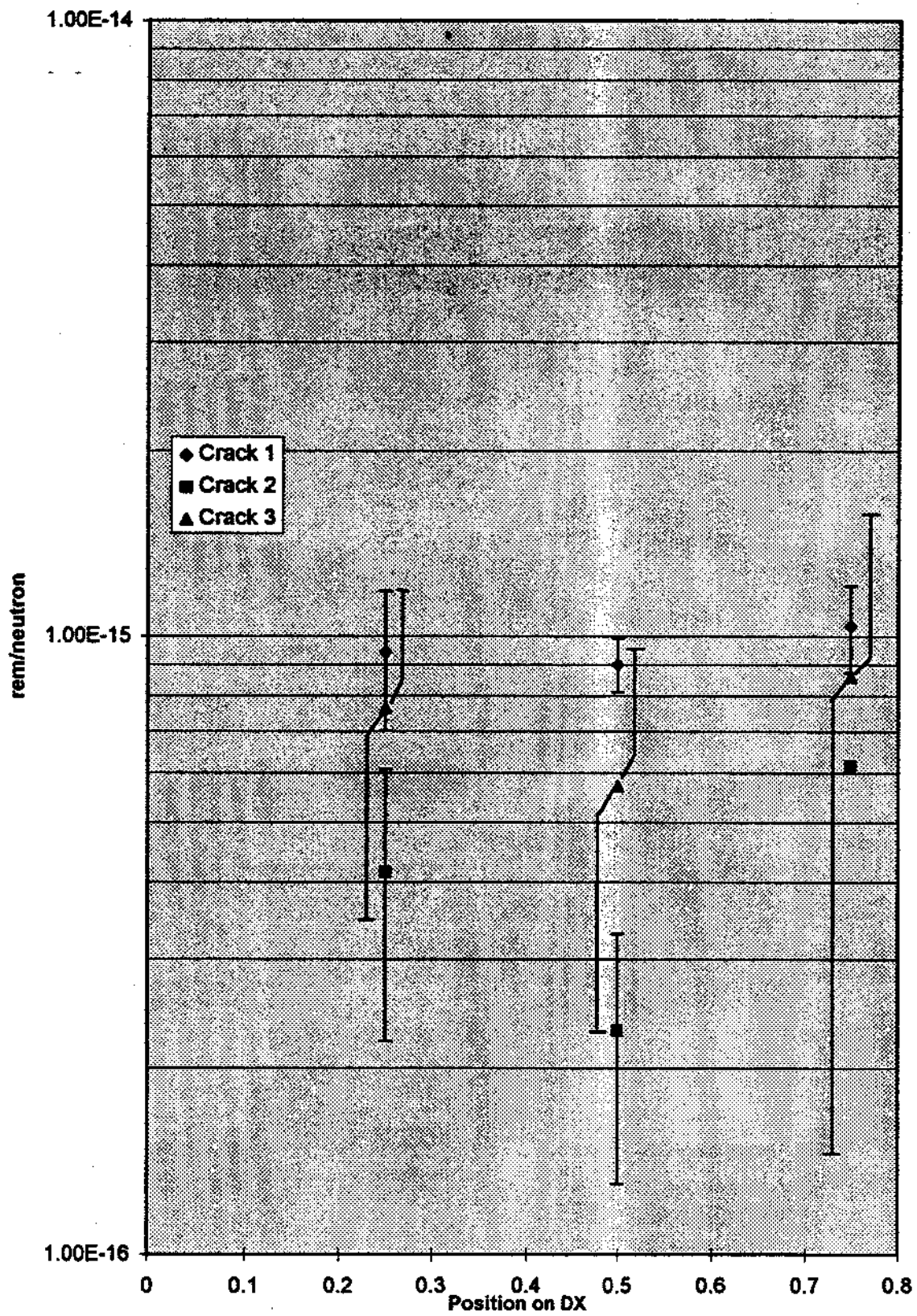


Fig. 2 Dose/Inc. vs. Position on DX for 3/8 " Radial Cracks

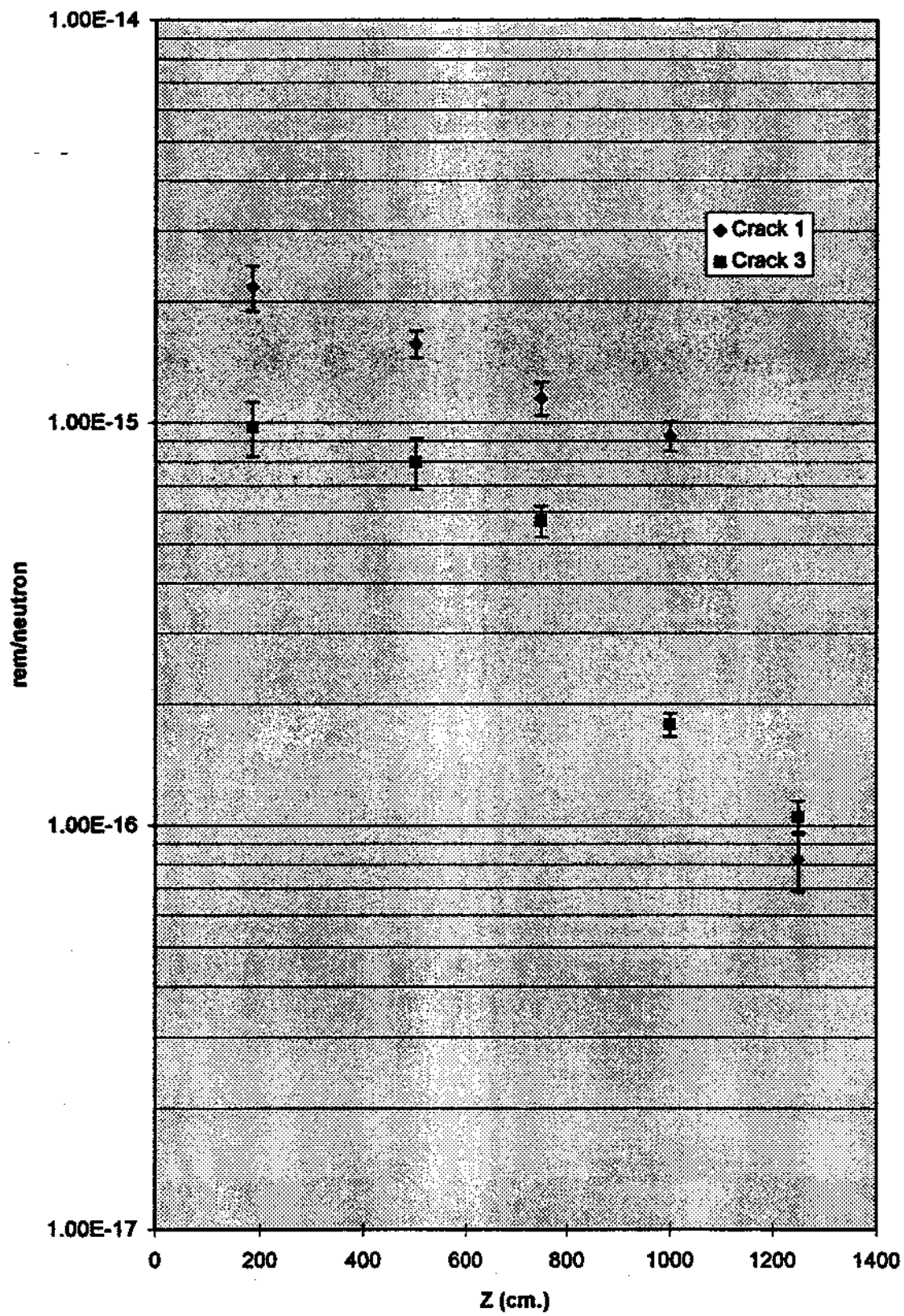


Fig. 3 Dose Exterior to 2 of the Cracks vs. Interaction Position (see text)

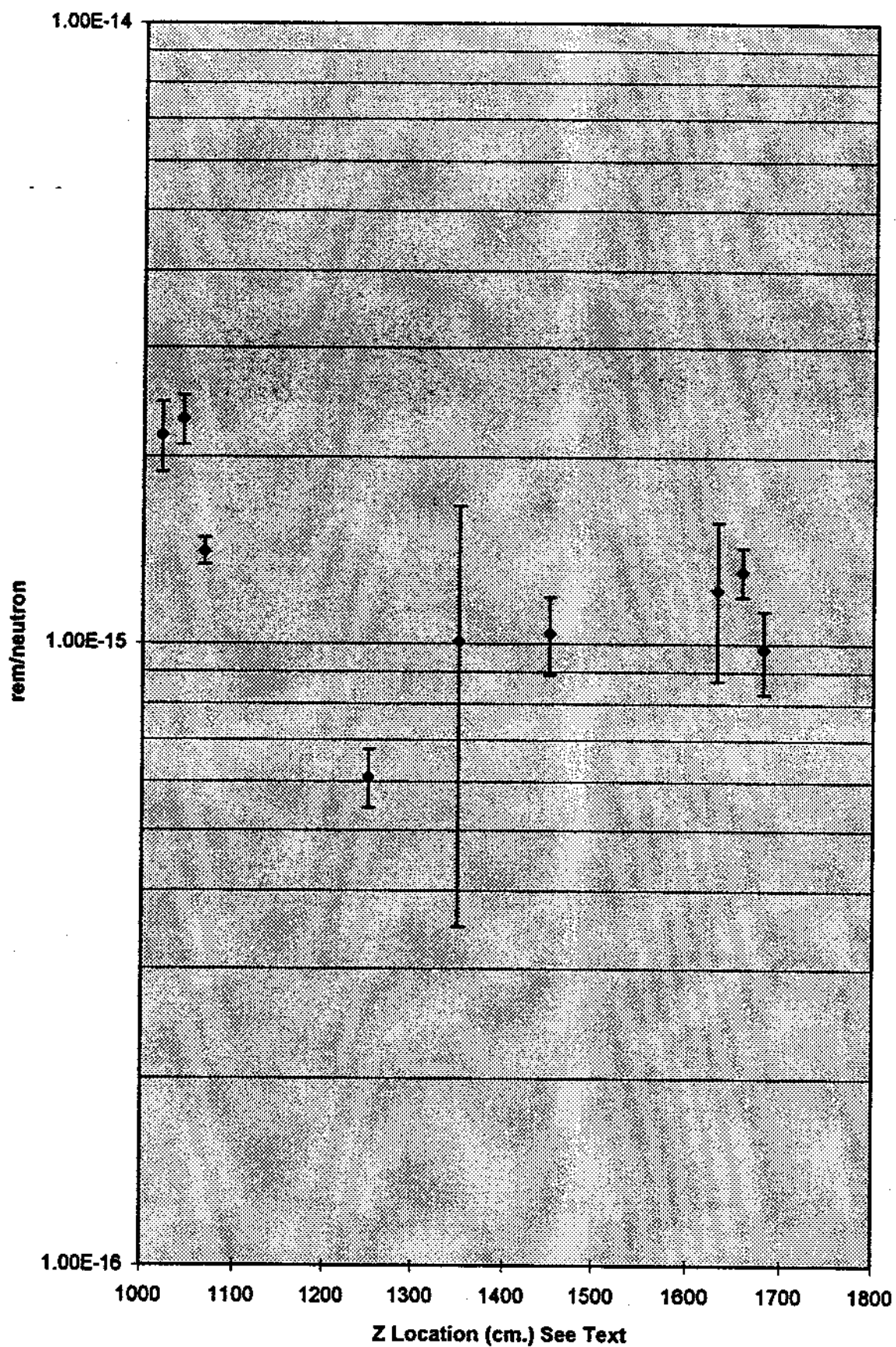


Fig. 4 Dose/Inc vs. Wall Position (1" radial cracks)

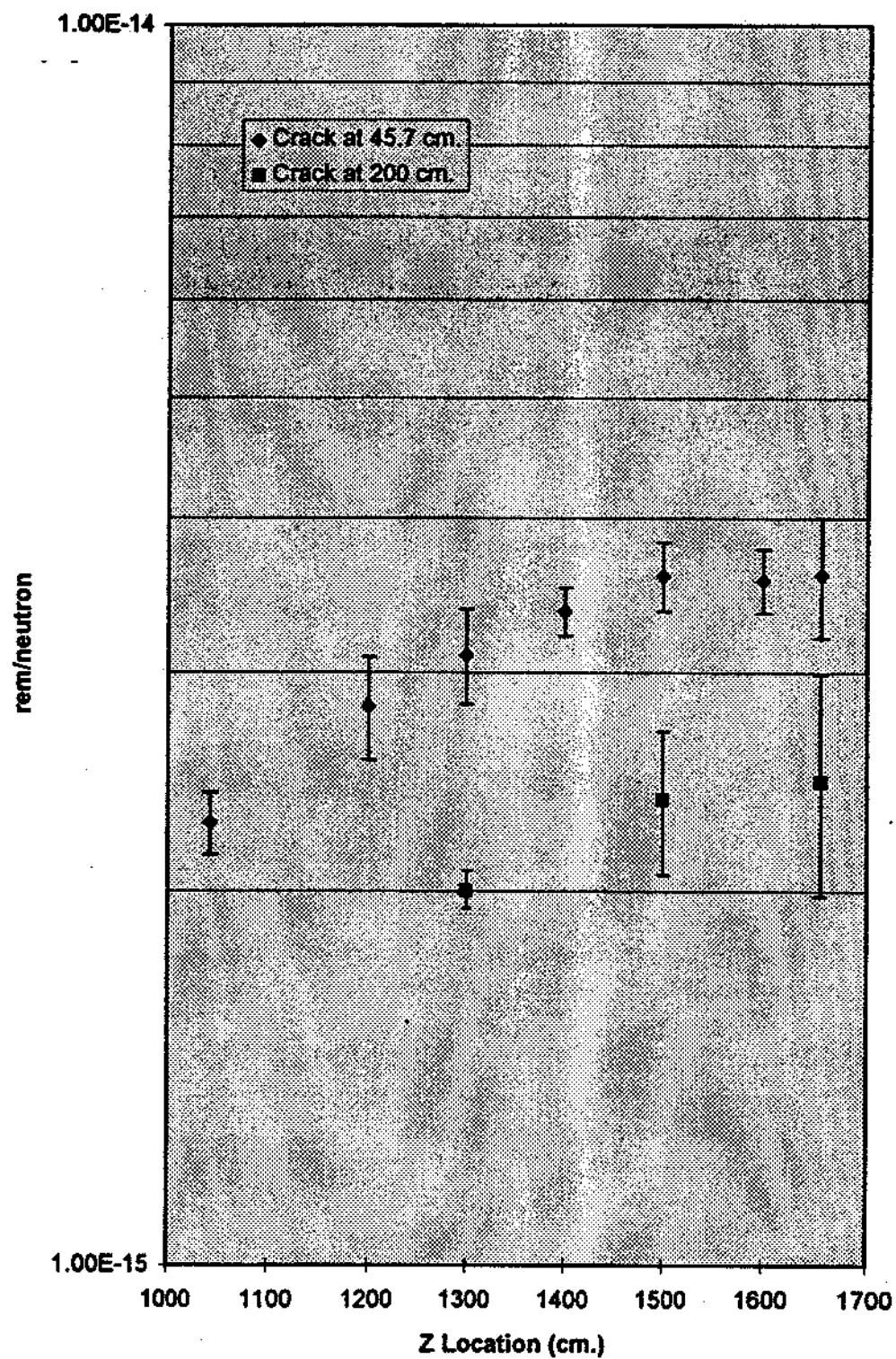


Fig. 5 Dose/Inc vs. Wall Position (1" horizontal cracks)

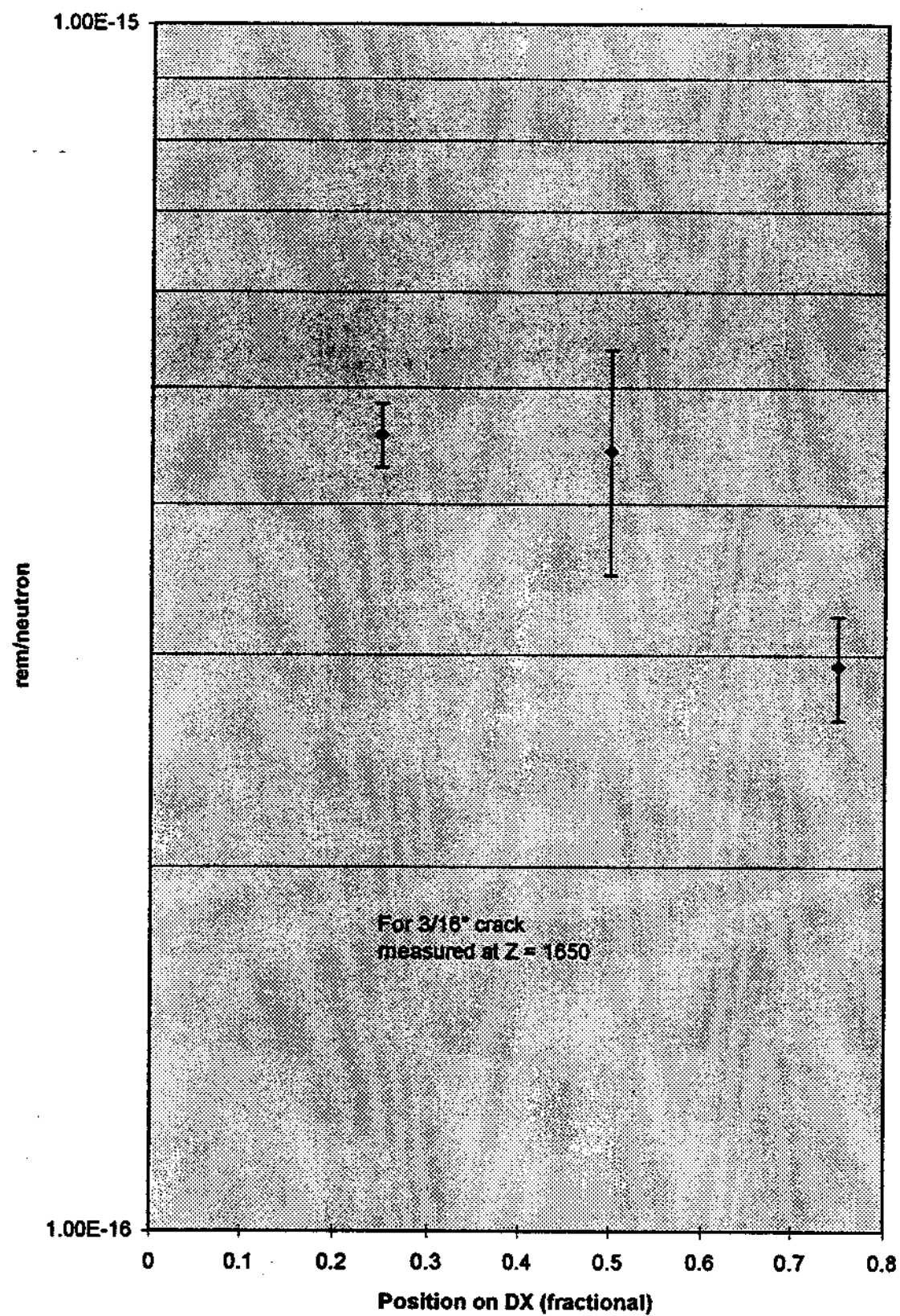


Fig. 6 Dose/Inc. vs. Position on DX for 3/16" Horizontal Crack

## Analysis of Cracks in the STAR Shield Wall

### I. Introduction

The approximation of the STAR Detector used to estimate the effects of cracks in the shield wall design dated 07/26/96 is shown in Fig. 1 below.

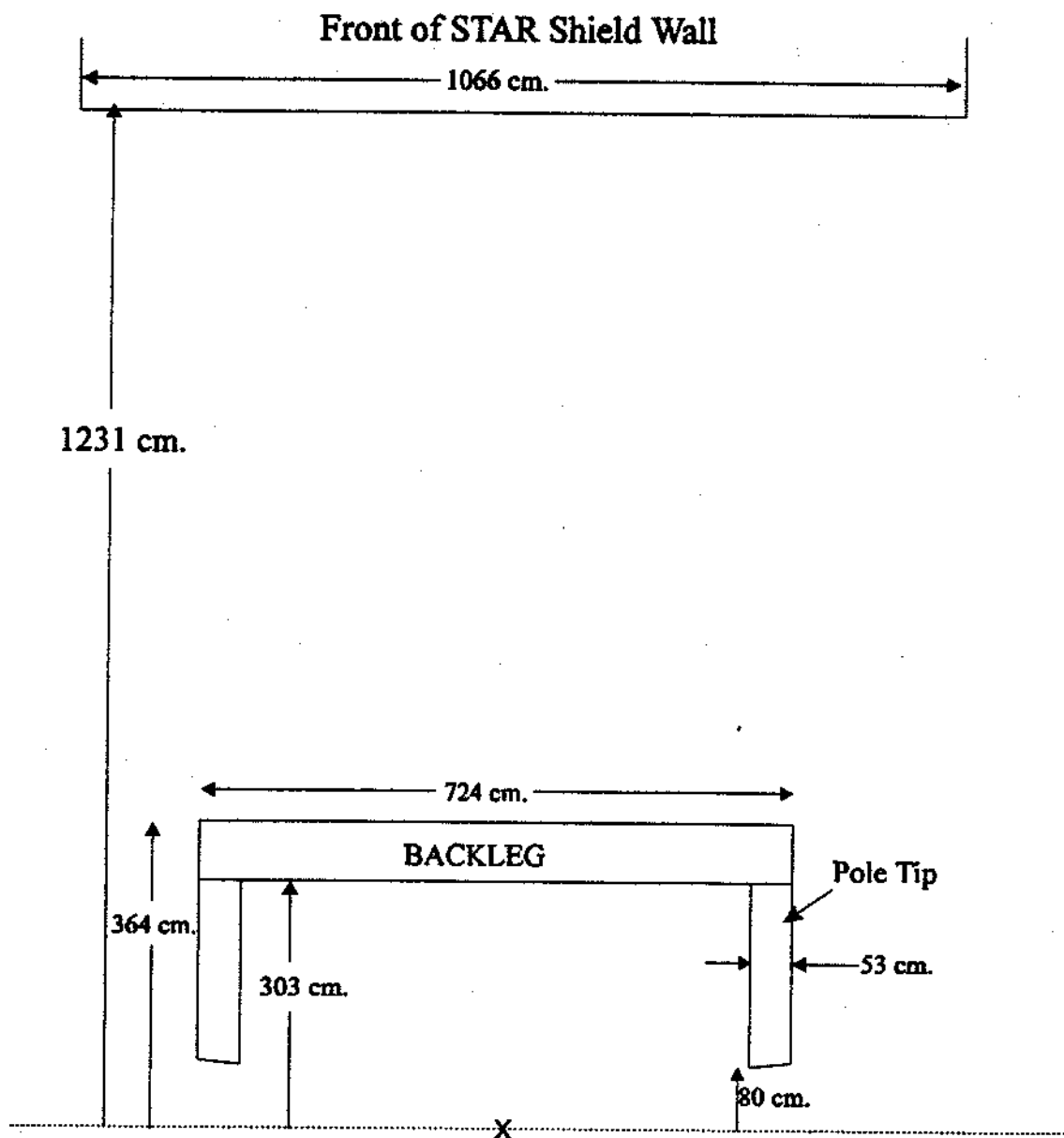


Fig. 1 Approximation of The STAR Detector

CASIM runs were made with a 5.5 ft. thick light concrete front shield wall, 3 ft. thick side walls, and a close approximation of the steel (treated as Fe) shown in Fig. 1. This simulates the material distribution on the midplane. For the canonical scraping loss on the DX magnet of a 250 GeV/c proton beam, the resulting maximum azimuthally averaged star density at the front and back of the wall was  $6.72 \times 10^{-8}$  and  $1.0 \times 10^{-9}$  respectively. With the design basis fault of  $1.14 \times 10^{13}$  protons (half beam at  $4 \times$  design), these star densities give 17.9 rem at the front of the wall and 267 mrem at the back. In obtaining these numbers, the star density is multiplied by 1.3 to account for a midplane enhancement caused by the magnetic field of DX and twice the "normal" star density to dose equivalent is used (e.g.,  $1.8 \times 10^{-5}$  rem/star/cc in concrete) for design purposes.

The 267 mrem, together with the 500 mrem criteria for radiation workers in a high occupancy region, gives the margin for the equivalent whole body dose due to cracks to be 233 mrem. The entrance dose of 17.9 rem multiplied by 0.85 gives 15.2 rem, which is the default incident low energy dose.<sup>1</sup>

In Section II below, the "high energy" contribution is estimated, i.e., the total excess dose due to cracks and hadrons greater than  $\sim 50$  MeV which interact in the shield wall. In Sections III and IV, the "low energy" contribution due to low energy neutrons incident on the wall is estimated assuming the default incident low energy dose. So-called "thick iron effects" which can increase the low energy contribution, are considered separately in Section V.

## II. The High Energy Contribution

### (A) Horizontal Cracks

The method for estimating the high energy contribution is described elsewhere.<sup>2</sup> The current shield wall design has a horizontal crack 8 inches above the accelerator midplane, about  $0.83^\circ$  from the beam line measured to the back of the wall. Unfortunately this is in a region where both the CASIM results and the parameterization of those results are changing very rapidly (See Fig. 4 of Ref. [2]) and the model underestimates the CASIM results. In this author's judgement, use of this model with a recommended safety factor of 2 (Ref. [1]) was not intended to apply to cracks which make an angle of less than about  $2^\circ$  with respect to the beam line. In the estimates presented here, a factor of 10 higher excess dose than given by the model in Ref. [1] is assumed for this crack. The next closest crack is 52 inches off the beam line, an angle of greater than  $5^\circ$ , where the dose is small and the recommended safety factor of 2 is quite reasonable.

The results of applying the model of Ref. [2] to these two cracks, with the assumed safety factors, are shown in Table 1 below. The entries are in mrem (whole body dose) for the canonical DX fault.

**Table 1 Estimate of the "High Energy" Contribution for Horizontal Cracks**

| Crack Width | Crack 8" Above<br>Beam Line | Crack 52" Below<br>Beam Line |
|-------------|-----------------------------|------------------------------|
| 1/16"       | 25                          | 0.8                          |
| 1/8"        | 108                         | 3.0                          |
| 3/16"       | 255                         | 6.8                          |

**(B) Vertical Cracks**

As described elsewhere<sup>3</sup>, an allowance of 20 mrem per 1/2 inch vertical crack in a 5 ft. thick wall is made. Assuming this scales linearly with the wall thickness gives 9, 18, and 27 mrem for cracks of 1/8, 1/4, and 3/8 inches respectively. A safety factor of 2 has been applied.

**III. Vertical Cracks (Low Energy Analysis)**

The obvious source for low energy neutrons impinging on the wall is the steel backleg shown in Fig. 1. As discussed in Ref. [1], for the purposes of estimating the attenuation through the wall, the assumption is made that evaporation from the outer 10 cm of this backleg dominate the dose. The CASIM star density for this region is shown in Fig. 2. The sharp peak is the exposed tip of the backleg in Fig. 1, and corresponds to a "short source" in the language of Ref. [1].

The attenuation as a function of position is obtained by adding the contributions from each  $\delta Z$  section of the backleg weighted by the star density at that position. The result is shown in Fig. 3 for a 1/8" crack.<sup>4</sup> The peak at the front edge of the backleg is  $6.9 \times 10^{-3}$ . For regions greater than 50 cm. from this position, an attenuation of  $2.0 \times 10^{-3}$  is assumed.<sup>5</sup> Now the "rules" of the analysis<sup>1</sup> are to apply twice this attenuation to the maximum entrance dose, but to divide the actual dose estimate by a factor of 3 to obtain the equivalent whole body dose. For the moment, applying this result to the default entrance dose of 15.2 rem gives the following table.

**Table 2. Excess Whole Body Dose For Default Normalization**

| Vertical Crack Size | Dose at Backleg Edge<br>(Equiv. Whole Body in<br>mrem) | Dose at Other Locations<br>(Equiv. Whole Body in<br>mrem) |
|---------------------|--|---|
| 1/8"                | 70   | 20  |
| 1/4"                | 140  | 41  |
| 3/8"                | 210  | 61  |

SD-outer 10 cm STAN Yoke

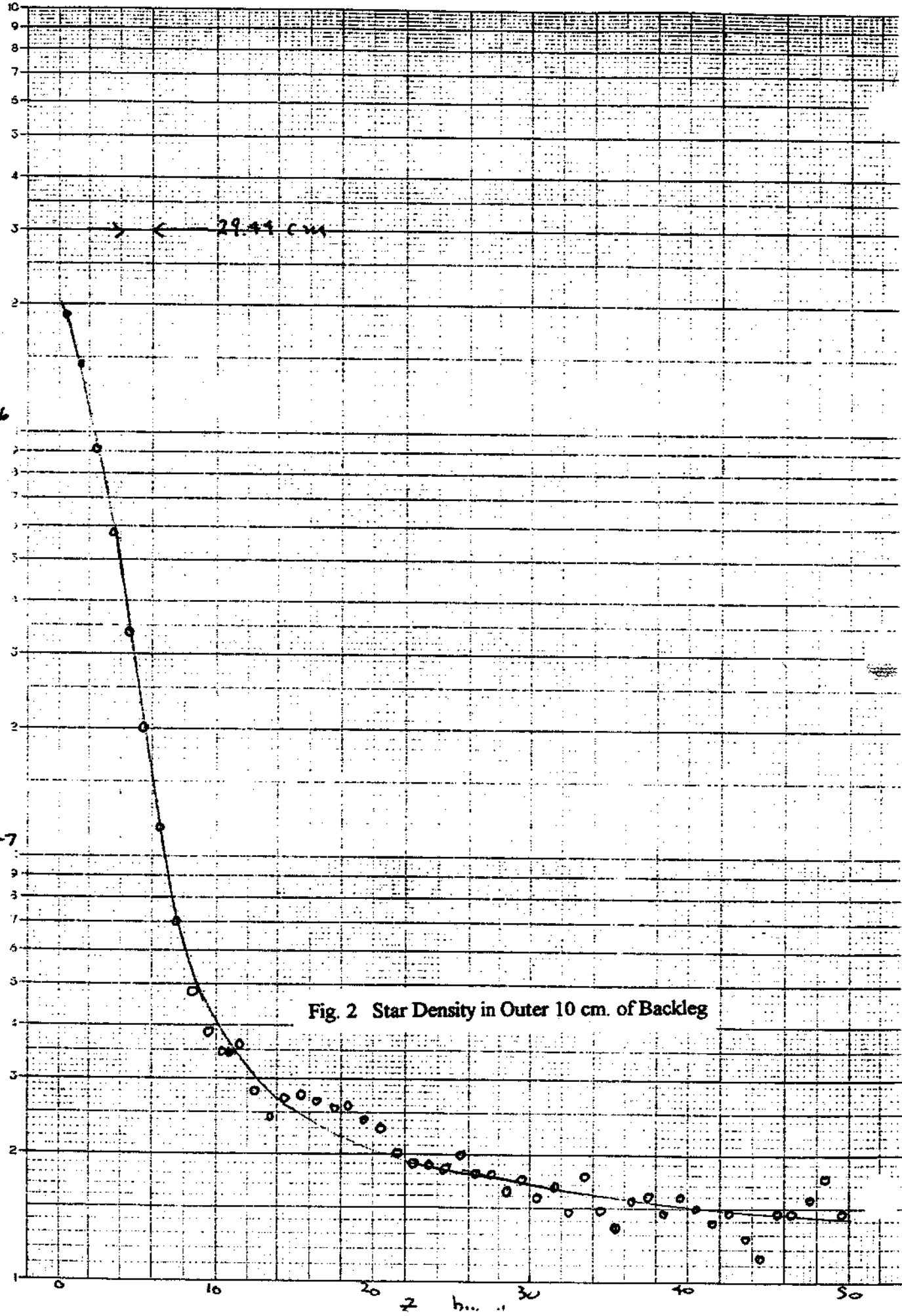
Stars/cm<sup>3</sup>-p

10<sup>6</sup>

10<sup>-7</sup>

29.41 cm

Fig. 2 Star Density in Outer 10 cm. of Backleg



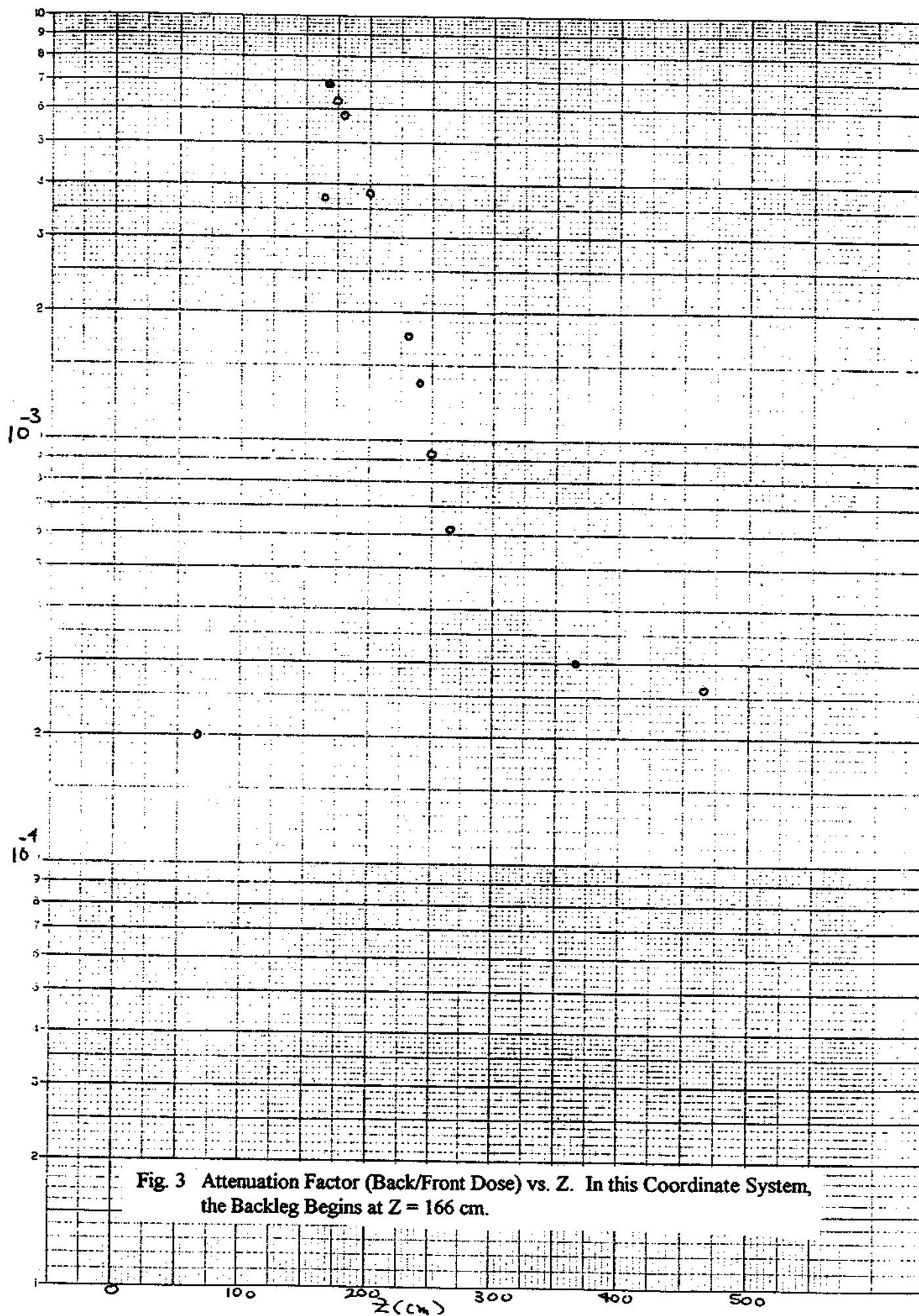


Fig. 3 Attenuation Factor (Back/Front Dose) vs.  $Z$ . In this Coordinate System, the Backleg Begins at  $Z = 166$  cm.

Evaluation of these results is deferred to Section VI because the possibility of enhancements to the default entrance dose must be discussed.

#### IV. Horizontal Cracks (Low Energy Analysis)

The low energy contribution to horizontal cracks is made by adding the contributions of some number of 5 cm. radius cylinders, in this case at the position of the outer part of the backleg, given a specific crack location. This is discussed in detail in Ref. [1]. Again, the model gives the attenuation through the wall and the result must be applied to an assumed low energy entrance dose. As described in Ref. [1], there is a certain amount of arbitrariness in the procedure because the entire entrance dose is assumed to come from some number of cylinders around the azimuth which was intended to be chosen in a "reasonable" manner. Here, the choice was made to add the contributions from 21 cylinders. The central one of these cylinders has its axis exactly aligned with the crack center and 10 additional cylinders are taken to be on either side. This gives an attenuation whose value is  $2.7 \times 10^{-3}$  for a 1/8" crack at both positions considered in Section II. This is higher than the value obtained in Ref. [1] (see Fig. 5 in Ref. [1]) because the source is farther away from the crack. With the default entrance dose and the "normal"  $\times 2$  safety factor, this gives an equivalent whole body dose of 14, 27, and 41 mrem for 1/16, 1/8, and 3/16 inch cracks respectively. Again, the actual excess dose obtained from the model is over a very small region and has been divided by 3 to obtain the "whole body equivalent."

#### V. "Thick Iron Effect"

A significant complication, discussed in Ref [1], is the "thick iron effect." This effect is most valid in a beam dump geometry. Consider such a geometry where a varying amount of pure Fe transverse shielding is imposed between the dump axis and the front of some concrete shield. As the Fe thickness is increased, the CASIM star density in the front of the concrete shield will decrease. However, the use of the equilibrium spectrum assumption to convert the star density to a dose equivalent will be increasingly incorrect as the Fe thickens because of a low energy ( $< 100$  KeV) "window" in Fe which causes an increased number of low energy neutrons in Fe relative to the number of high energy hadrons. Based on calculations by Gollon,<sup>6</sup> the low energy dose is .85 of the total CASIM dose obtained with an equilibrium spectrum assumption for "thin iron" (28 cm.) but rises to 2.0 times this dose for Fe 100 cm. thick.

However, the actual geometry is not that of a beam dump. Other than the relatively short pole tips shown in Fig. 1, the backleg thickness shown in Fig. 1 is 2 ft. If this is changed to a 1 ft. thickness in CASIM, the shield wall entrance star density does not change.<sup>7</sup> On the other hand, the method of estimation is crude and is difficult to defend unless at least some degree of conservatism is employed at each step. In this spirit some allowance should be made for the possibility of thick iron effects. The allowance made here is the *square root* of an enhancement factor based on Gollon's two numbers.<sup>8</sup> This factor is 2.4 over the relatively narrow region of the poles (where the thickness is 284 cm.) and 1.27 over the rest of the backleg (61 cm. Fe).

## VI. Summary of Results

With the normalization allowance discussed immediately above, the results of the preceding analysis is summarized in Table 3 below. Note that vertical cracks in the (narrow) pole tip region are affected both by the "hot-spot" attenuation ratio and the largest allowance for thick iron.

**Table 3. Results With Recommended Allowance for Normalization Enhancements**  
(Entries in Equivalent of Whole Body Dose@ 4x Design Intensity)

| <b>Case: Horizontal Crack 8" From Beam Line</b> |               |                         |                                |                         |                                |
|---|---------------|-------------------------|--------------------------------|-------------------------|--------------------------------|
| <b>Crack Size (inches)</b>                      | <b>High E</b> | <b>Low E (Pole Tip)</b> | <b>Low E (Not at Pole Tip)</b> | <b>Total (Pole Tip)</b> | <b>Total (Not at Pole Tip)</b> |
| 1/16  | 25            | 34                      | 18                             | 59                      | 43                             |
| 1/8   | 108           | 65                      | 34                             | 173                     | 142                            |
| 3/16  | 255           | 98                      | 52                             | 353                     | 307                            |
| <b>Case: Other Horizontal Cracks</b>            |               |                         |                                |                         |                                |
| 1/16  | 0.8           | 34                      | 18                             | 35                      | 19                             |
| 1/8   | 3.0           | 65                      | 34                             | 68                      | 37                             |
| 3/16  | 6.8           | 98                      | 52                             | 105                     | 59                             |
| <b>Case: Vertical Cracks</b>                    |               |                         |                                |                         |                                |
| 1/8   | 9             | 168                     | 25                             | 177                     | 34                             |
| 1/4   | 18            | 336                     | 52                             | 354                     | 70                             |
| 3/8   | 27            | 504                     | 77                             | 531                     | 104                            |

The entries in Table 3 should be compared with the margin of 233 mrem. The horizontal crack near the beam line has difficulty at some width between 1/8" and 3/16". This is mostly due to the "high energy" component. Vertical cracks have difficulty only in the region of the pole tip, due to the allowance for normalization enhancement proposed. In regard to the last conclusion, it should be noted that only a very limited region of space in the vertical direction has difficulty. This is because, when the detector is in the collision hall, occupancy behind the shield wall becomes low for elevations higher than ~ 6 ft. off the floor. Occupancy becomes high at higher elevations only when the detector is in the assembly area which implies that the source for normalization enhancement has been removed.

At the time of this writing the STAR collaboration has agreed to test the feasibility of "sealing" the horizontal crack near the beam line by inserting a thin layer of foam between the blocks at this position.

Since the problem with vertical cracks affects only a very limited extent of the wall, two local "shields" might well be employed. Fig. 4 shows that about 3" of CH<sub>2</sub> (the equivalent of water in the figure) reduces the estimated dose for a 3/8" crack to the required level.

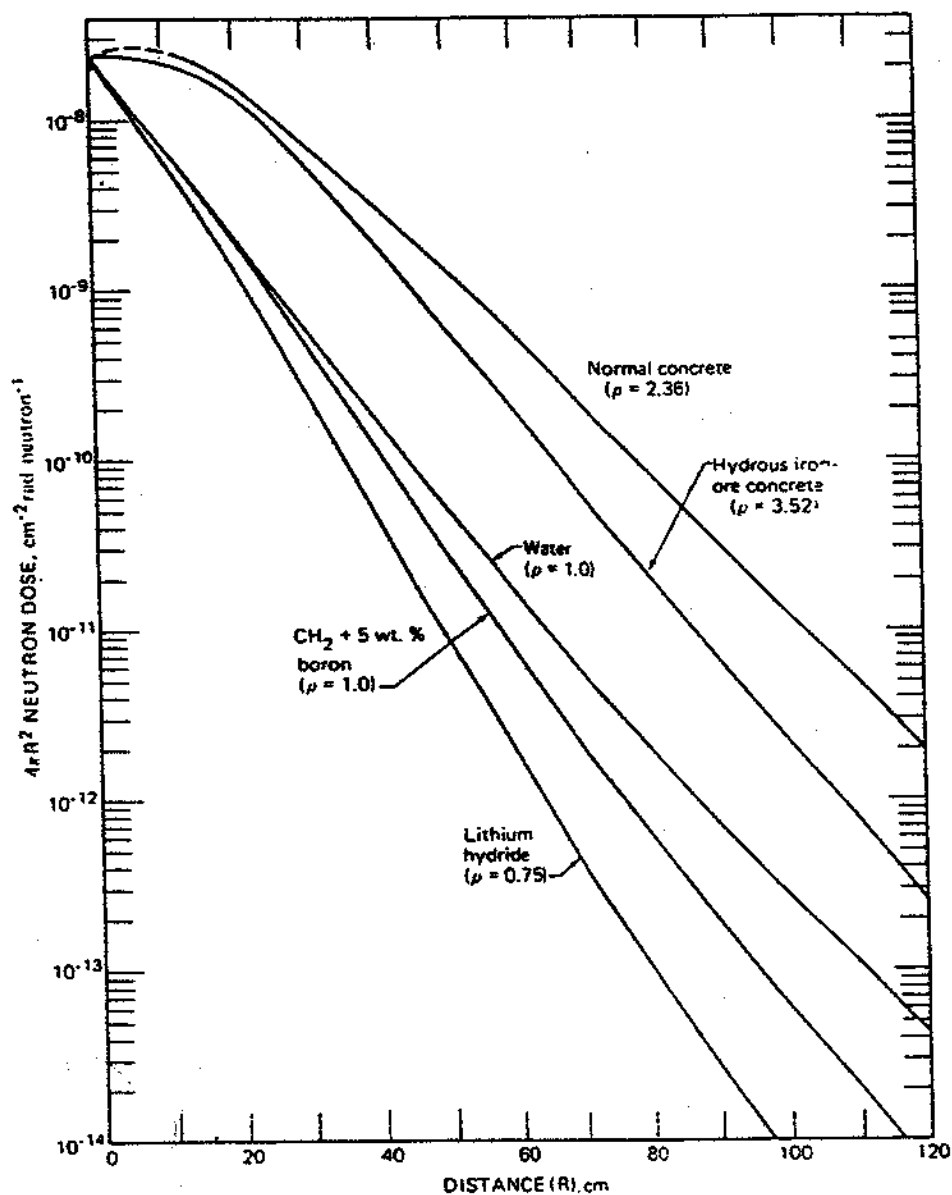


Fig. 8.12—Neutron dose vs. depth in the indicated materials fission-neutron source. (Based on data from Nichols<sup>47</sup> and Kam and Clark.<sup>48</sup>)

Fig. 4. From the Reference Indicated

### References/Footnotes

1. A.J. Stevens, "Approximation for Low Energy Dose Through Cracks in Shielding Walls," RHIC/DET Note 21, June, 1996.
2. A.J. Stevens, "Estimate of High Energy Punch-Through in Shielding Wall Cracks," AD/RHIC/RD-98, April, 1996.
3. Memorandum from A.J. Stevens to S. Musolino dated 05/08/96, subject: "High Energy Punch-Through in Vertical Shielding Wall Cracks."
4. The attenuation factor is linear with crack width.
5. This is the value at 50 cm from the peak. Although the attenuation ratio in Fig. 3 is very much smaller than this at significantly larger distances, some allowance should be made for the possibility (probability) that the CASIM star density exaggerates the peak dose. An exaggeration of the ratio at one position will imply a suppression at other positions. If a uniform star density were assumed instead of that shown in Fig. 2, the ratio turns out to be  $7 \times 10^{-4}$ . Allowing  $2 \times 10^{-3}$  amounts to taking the model seriously when it gives a conservative result and making a conservative allowance when it does not.
6. P.J. Gollon, "Shielding of Multi-Leg Penetrations into the RHIC Collider," AD/RHIC/RD-76 (1994) and private communication.
7. The most relevant steel thickness is likely to be the yoke of DX which is certainly "thin."
8. Specifically, the enhancement factor is assumed to be the square root of a number derived from the assumption of linearity between 1.0 at 28 cm., and 2.35 (2/.85) at 100 cm. Another way of looking at this is that the allowance for an enhancement is the *geometric mean* of no enhancement and a linear enhancement.